HPVP-GTAW 电弧力及焊接质量分析

从保强[1]， 齐铂金[1]， 杨明轩[1]， 李 伟[1,2]， 王乐笑[1*]
(1. 北京航空航天大学 机械工程及自动化学院，北京 100191；2. 北京石油化工学院 电气工程系，北京 102617)


从保强

摘 要：分别以3种不同材质铝合金平板材料为试验对象，研究分析了复合超高频脉冲方波变极性钨极氩弧焊接(HPVP-GTAW)过程中电弧力的变化及其对焊缝成形特征和接头力学性能的影响. 结果表明，与常规变极性氩弧焊工艺相比，脉冲方波电流的加入使得HPVP-GTAW电弧力显著增加，同时焊缝熔透率大幅提高，接头力学性能得到明显改善和提高；保持脉冲电流幅值和占空比基本不变，在10～80 kHz范围内，脉冲电流频率对焊接过程产生了重要影响，频率为40 kHz时，HPVP-GTAW电弧力和焊缝熔透率均达到最大，分别约为常规变极性焊接电弧的1.9倍和1.7倍.

关键词：超高频脉冲电流；变极性钨极氩弧焊；电弧力；焊接质量
中图分类号：TG457.14 **文献标识码**：A **文章编号**：0253－360X(2013)01－0021－04

0 序 言

复合超高频脉冲方波变极性钨极氩弧焊接技术(hybrid pulse variable polarity gas tungsten arc welding，HPVP-GTAW)是一种优质高效的新型电弧焊接工艺方法，该工艺在电流极性快速变换($di/dt \geqslant 50$ A/μs)的基础上，在单极性期间加入百安培以上的高频脉冲方波电流(脉冲频率≥20 kHz)[1]，将其用于铝合金材料的焊接加工，初步研究结果表明，超高频脉冲方波电流的加入对不同材质铝合金焊缝组织结构和接头力学性能均会产生重要影响，并可明显改善和提高铝合金的电弧焊接质量[2,3].

目前国内外有关HPVP-GTAW焊接过程中超高频脉冲方波电流作用机制的研究开展甚少，文中从焊接电弧力特性的角度出发，研究不同脉冲电流频率条件下电弧力的变化规律以及对应焊缝成形特征和接头性能的变化，研究结果可为进一步优化HPVP-GTAW焊接过程参数并提高铝合金的电弧焊接质量提供依据，具有重要的应用价值.

1 试验方法

试验内容主要包括焊缝成形特征、电弧力测试以及焊接接头力学性能检测共3个部分.

收稿日期：2011－11－22
基金项目：国家自然科学基金资助项目(50975015，51005011)
* 参加此项研究工作的还有杨 舟，李玉龙

1.1 焊缝成形特征

试件选择厚度为5.5 mm的2A14-T6铝合金平板，尺寸规格为120 mm×60 mm. 焊缝填充焊丝选用直径为2.4 mm的ER2319. 试验采用平板堆焊工艺，为保证获得良好的堆焊焊缝成形，电弧成功引燃定点燃烧约10 s后由焊接控制平台控制焊枪匀速移动，图1a为实际获得的焊缝正面外观. 沿垂直于焊接方向，分别在焊缝不同位置截取3处断面，使用游标卡尺(精确度为0.02 mm)分别测量3处横截面的熔深和熔宽(图1b中B和H分别代表焊缝熔宽和熔深). 取3次测量结果的平均值以减小误差，并计算得出焊缝熔透率R(用熔深H与熔宽B的比值表征)，以此来衡量HPVP-GTAW焊缝的成形特征.

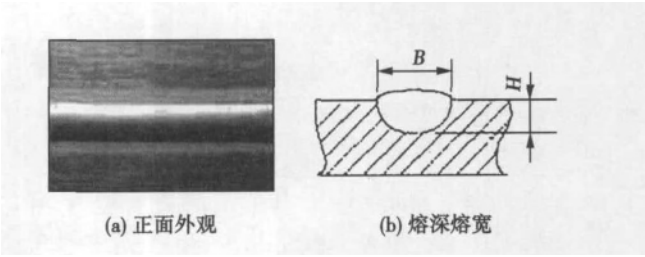

图1 焊缝成形示意图
Fig. 1 Schematic diagram of weld formation

1.2 电弧力测试

试件选择厚度为4 mm的2219-T87铝合金平板，尺寸规格为100 mm×50 mm. 基于由精密测力传感器和轻质支架式焊接平台构建的电弧力测量平台，采用电弧定点燃烧方法，完成对HPVP-GTAW电

弧力的测量.

1.3 接头力学性能

试件选择厚度为 4 mm 的 2219-T87 和 3 mm 的 5A06-O 铝合金平板,尺寸规格为 200 mm × 100 mm,焊接长度为 200 mm,I 形接头,焊缝填充焊丝选用直径为 2.4 mm 的 ER2319(用于 2219-T87)和 ER5356(用于 5A06-O). 沿垂直于焊缝的方向切取金相试样,使用 Keller 试剂(HNO_3 2.5 mL,HCl 1.5 mL,HF 1 mL,H_2O 95 mL)对抛光试样进行化学浸蚀,在 BX51M 光学显微镜下观察并测量焊缝熔合区的宽度. 焊态条件下,采用线切割垂直于焊接方向切取拉伸试样,每组工艺制取 3 个试样,并在 DWD-50E 型电子拉伸试验机上进行拉伸试验,拉伸速度为 2 mm/min.

上述铝合金试件在焊前均先用丙酮有机溶剂擦拭去除表面油污,然后采用化学清理方法(10% NaOH + 15% HNO_3)去除表面氧化膜. 采用机械清理方法去除填充焊丝表面的氧化膜. 试验采用的焊接电流波形如图 2 所示.

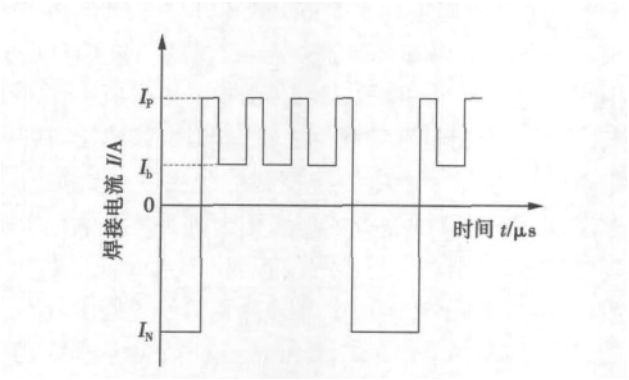

图 2 HPVP 电流波形示意图

Fig. 2 Schematic diagram of HPVP current waveform

1.4 焊接工艺参数

文中主要研究脉冲电流频率对 HPVP-GTAW 电弧力等方面的影响,各部分试验采用的主要焊接工艺参数如下.

(1) 焊缝成形测试. 基值电流 I_b = 80 A,峰值电流 I_P = 160 A,负极性电流 I_N = 180 A,保护氩气流量 q_{Ar} = 15 L/min,焊接速度 v_1 = 180 mm/min,送丝速度 v_2 = 190 mm/min,对应常规 VP-GTAW 正极性焊接电流为 130 A.

(2) 电弧力测试. I_b = 70 A,I_P = 145 A,I_N = 140 A,q_{Ar} = 15 L/min,对应常规 VP-GTAW 正极性焊接电流为 115 A.

(3) 2219-T87 接头性能测试. I_b = 95 A,I_P = 155 A,I_N = 195 A,q_{Ar} = 15 L/min,v_1 = 120 mm/min,v_2 = 150 mm/min,对应常规 VP-GTAW 正极性焊接电流为 155 A.

(4) 5A06-O 接头性能测试. I_b = 60 A,I_P = 130 A,I_N = 120 A,q_{Ar} = 15 L/min,v_1 = 150 mm/min,v_2 = 150 mm/min,对应常规 VP-GTAW 正极性焊接电流为 100 A.

其它焊接工艺参数分别为变极性频率 0.1 kHz;正负极性电流持续时间比 8∶2;脉冲电流频率在 0 ~ 80 kHz 范围内取 0,10,20,40,60 kHz 和 80 kHz 共 6 个水平,占空比 50% 不变. 电极选用直径为 3 mm 的 WC20,电极高度为 3 mm.

2 试验结果与分析

2.1 焊缝熔透成形

2A14-T6 铝合金 HPVP-GTAW 焊缝熔宽 B、熔深 H 与熔透率 R 的测试结果如表 1 所示,熔透率 R 与脉冲电流频率 f_H 之间的变化关系曲线如图 3 所示,未加入脉冲电流以及采用不同脉冲电流频率焊缝试样的横截面如图 4 所示.

表 1 焊缝成形测试结果

Table 1 Experimental results of weld formation

序号	脉冲电流频率 f_H/kHz	熔宽 B/mm	熔深 H/mm	熔透率 R(%)
1	0	7.2	1.8	25
2	10	7.2	2.6	36
3	20	7.5	2.4	32
4	40	8.2	3.5	43
5	60	7.8	2.8	36
6	80	7.4	2.2	30

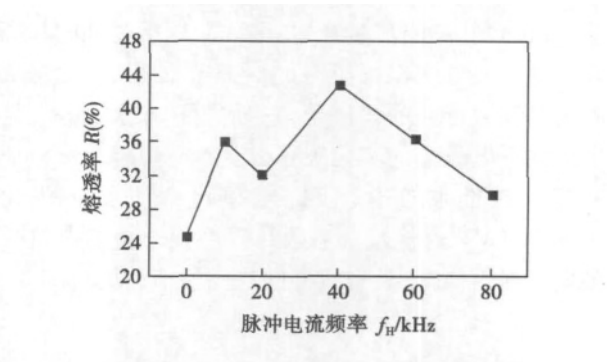

图 3 焊缝熔透率与脉冲电流频率变化曲线

Fig. 3 Variation of weld penetration with pulse frequency

从表 1 和图 3 中可以明显看出,常规 VP-GTAW 焊缝熔透率仅为 25%(图 4a),脉冲方波电流的加入对焊缝成形产生了显著影响,并可明显提高铝合金焊缝的熔透率(R 最小增加量约为 20%),脉冲电

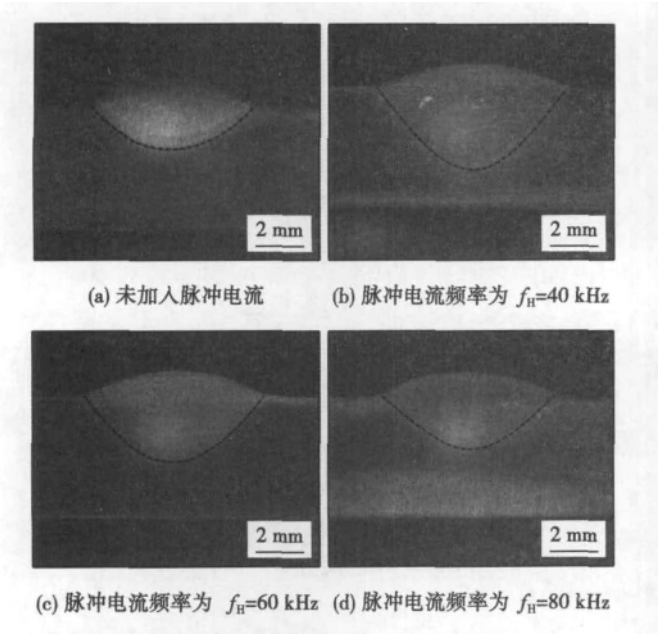

图 4　焊缝横截面对比

Fig. 4　Comparison of weld formation

流频率 f_H = 40 kHz 时，焊缝熔透率达到最大（图 4b，R = 43%）.

2.2　电弧力

图 5 所示为 2219-T87 铝合金 HPVP-GTAW 电弧力 F_a 与超高频脉冲方波电流频率 f_H 之间的变化关系曲线. 从实际测试结果可以得出，与未加入脉冲方波电流相比（F_a = 5.2 mN），脉冲方波电流的加入可明显提高 F_a 的大小（F_a 最小增加量约为 25%），且脉冲电流频率 f_H 对 F_a 具有显著影响. 当 f_H 处于 20 kHz 以下时，F_a 在 5 kHz 时达到一个较高水平（F_a = 7.5 mN），这与国内学者的研究结果基本一致[4]；当 f_H 超过 20 kHz 时，F_a 则又明显增加，在 f_H = 40 kHz 时达到最大，为 9.7 mN.

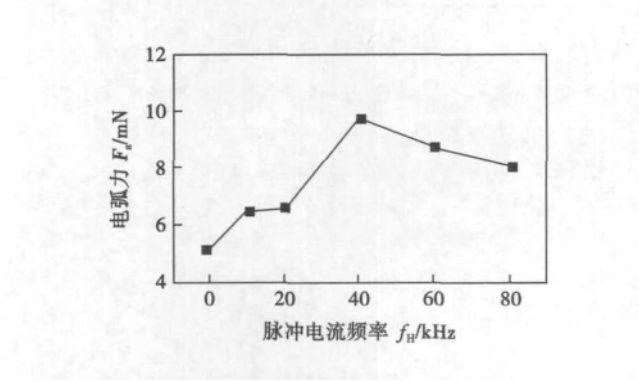

图 5　电弧力与脉冲电流频率变化曲线

Fig. 5　Variation of arc pressure with pulse frequency

2.3　接头力学性能

5A06-O 和 2219-T87 焊接接头抗拉强度 R_m 与 f_H 之间的变化关系曲线如图 6 所示，可以看出，对于 5A06-O 和 2219-T87 两种铝合金材料，与常规变极性焊接工艺相比，采用 HPVP-GTAW 焊接工艺均可明显提高其焊接接头的拉伸力学性能[5,6]. 当 f_H = 40 kHz 时，对应 5A06-O 和 2219-T87 焊接接头抗拉强度分别提高约 13% 和 15%.

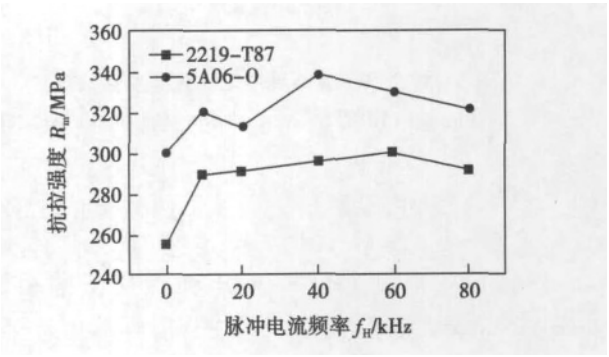

图 6　抗拉强度与脉冲电流频率变化曲线

Fig. 6　Variation of tensile strength with pulse frequency

对比不同脉冲电流频率条件下 HPVP-GTAW 焊接电弧力 F_a、焊缝熔透率 R 以及接头抗拉强度 R_m 的变化曲线，可以发现 F_a，R 和 R_m 三者与 f_H 之间的变化规律具有较好的一致性，即在文中试验条件下，当 f_H = 40 kHz 时，F_a，R 和 R_m 基本均达到最大值，且随着 f_H 大小的改变，F_a，R 和 R_m 的变化规律亦趋于一致. 分析认为，一方面电弧力的主要来源是电磁力和等离子流力，高频脉冲方波电流的加入可使焊接电弧产生高频效应，在焊接电弧内部，脉冲电流与自激产生的脉动变化的磁场相互作用，使得焊接电弧沿径向发生收缩，导致电弧内电磁力和等离子流力均发生改变，最终使焊接电弧力发生显著变化[7,8]；另一方面在实际焊接过程中，超高频脉冲方波电流经由电弧负载流入熔池后，在熔池内部产生电磁场效应，熔池液态金属在外部电弧压力和内部感应电磁力的共同作用下，焊缝熔池液态金属将产生强烈的复杂规律性流动，熔池液态金属流动性的增强既有利于焊缝熔池内部热量的传导，同时又对焊缝熔合区部位的冲刷作用显著加强，使得焊缝熔合区的宽度明显减小，如图 7 所示，2219-T89 铝合金与常规 VP-GTAW 焊接工艺（W = 520 μm）相比，当 f_H 超过 20 kHz 时，HPVP-GTAW 焊缝熔合区宽度 W 显著减小，W 最小减少量约为 38%，熔合部位部分未熔化的高效形核质点被卷入焊缝中心区域[9,10]，有助于焊缝金属结晶组织结构的细化，从而最终达到改善和提高铝合金焊接接头力学性能的效果.

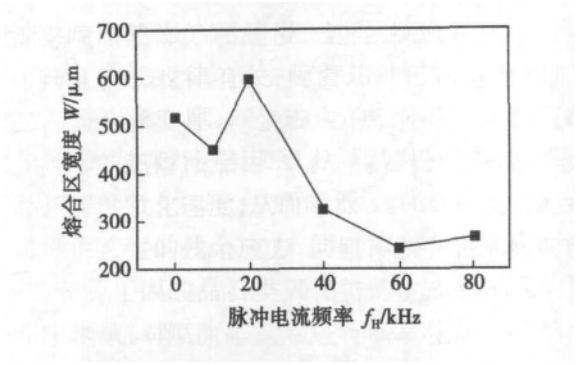

图7 熔合区宽度与脉冲电流频率变化曲线

Fig. 7 Variation of fusion zone width with pulse frequency

3 结 论

(1) 与常规 VP-GTAW 电弧焊接工艺相比，HPVP-GTAW 焊接电弧力明显提高，焊缝熔透率显著增加，接头力学性能得到明显改善和提高，同时脉冲方波电流频率对 HPVP-GTAW 电弧力、焊缝熔透率和接头力学性能均具有显著的影响.

(2) 保持脉冲占空比 50% 不变，脉冲电流频率为 40 kHz 时，HPVP-GTAW 焊接电弧力和焊缝熔透率均达到最大，与常规 VP-GTAW 焊接相比，分别增加约 90% 和 70%.

参考文献:

[1] 从保强，齐铂金，周兴国，等. 铝合金超快变换复合脉冲方波 VPTIG 焊接技术 [J]. 焊接学报，2009，30(2)：25－28.
Cong Baoqiang，Qi Bojin，Zhou Xingguo，*et al*. Ultrafast-convert complex ultrasonic pulse square wave VPTIG arc welding technology of aluminum alloy [J]. Transactions of the China Welding Institution，2009，30(2)：25－28.

[2] 从保强，齐铂金，周兴国，等. 超音频脉冲方波电流参数对 2219 铝合金焊缝组织和力学性能的影响 [J]. 金属学报，2009，45(9)：1057－1062.
Cong Baoqiang，Qi Bojin，Zhou Xingguo，*et al*. Influences of ultrasonic pulse square-wave current parameters on microstructures and mechanical properties of 2219 aluminum alloy weld joints [J]. Acta Metallurgica Sinica，2009，45(9)：1057－1062.

[3] 从保强，齐铂金，李 伟，等. 脉冲电流频率对 2219 铝合金焊缝组织性能的影响 [J]. 焊接学报，2010，31(9)：37－40.
Cong Baoqiang，Qi Bojin，Li Wei，*et al*. Effect of pulse current frequency on microstructure and mechanical properties of 2219 aluminum alloy weld joints [J]. Transactions of the China Welding Institution，2010，31(9)：37－40.

[4] 邱 灵，范成磊，林三宝，等. 高频脉冲变极性焊接电源及电弧压力分析 [J]. 焊接学报，2007，28(11)：81－85.
Qiu Ling，Fan Chenglei，Lin Sanbao，*et al*. High frequency pulse modulated variable polarity welding power and its arc pressure [J]. Transactions of the China Welding Institution，2007，28(11)：81－85.

[5] 从保强. 高强铝合金快速变换复合脉冲变极性 TIG 焊接技术研究 [D]. 北京：北京航空航天大学，2009.

[6] 从保强，齐铂金，周兴国，等. 复合脉冲方波电流频率对 5A06 铝合金焊缝组织和性能的影响 [J]. 焊接学报，2010，31(1)：89－92.
Cong Baoqiang，Qi Bojin，Zhou Xingguo，*et al*. Effect of complex-pulse square-wave current frequency on microstructure and mechanical properties of 5A06 aluminum alloy welds [J]. Transactions of the China Welding Institution，2010，31(1)：89－92.

[7] 赵家瑞，李义丹. 高频脉冲 TIG 焊的电弧控制及高频效应 [J]. 天津大学学报，1989(3)：25－32.
Zhao Jiarui，Li Yidan. Control over arc of pulsed high frequency TIG welding and high frequency effect [J]. Journal of Tianjin University，1989(3)：25－32.

[8] CookG E，Eassa E H. The effect of high-frequency pulsing of a welding arc [J]. IEEE Transactions on Industry Applications，1985，1A－21(5)：1294－1299.

[9] Gutierrez A，Lippold J C. A proposed mechanism for equiaxed grain formation along the fusion boundary in aluminium-copper-lithium alloy [J]. Welding Journal，1998，77(3)：123s－132s.

[10] Lin D C，Wang G X，Srivatsan T S. A mechanism for the formation of equiaxed grains in welds of aluminium-lithium alloy 2090 [J]. Materials Science and Engineering A，2003，351：304－309.

作者简介: 从保强，男，1979 年出生，博士，讲师. 主要研究方向为特种电弧焊接技术、焊接过程控制、新型弧焊电源技术及应用等. 发表论文 30 余篇. Email: congbq@buaa.edu.cn

通讯作者: 齐铂金，男，教授. Email: qbj@buaa.edu.cn

ence and Technology, Changchun 130022, China). pp 17 – 20

Abstract: The distributions of the elements in CO_2 laser-metal active gas (MAG) hybrid welding were investigated with scanning electron microscope. The relation between the forming process of weld and the distribution of the element in CO_2 laser-MAG hybrid welding process was analysed with high-speed camera and scanning electron microscope. Both the melting metal flow and position of adding elements decide the element distributions. Metal flow varies due to changes of DLA (distance between laser and arc). The fluctuation of the keyhole can promote the uniform distribution of the element, but the impactness of the metal vapour enriches element in local zone of welding pool. The scanning and stiring of laser beam further make the uniform element distribution. The highest content and uniform distribution of elements can be obtained in the molten pool when the distance between laser and arc is 3 mm and elements are added from the location 1.0 mm away from the surface.

Key words: CO_2 laser-arc hybrid welding; melting metal flow; element distribution

Analysis of arc pressure and its weld quality in hybrid ultra-high frequency pulse VP-GTAW process CONG Baoqiang[1], QI Bojin[1], YANG Mingxuan[1], LI Wei[1,2], WANG Lexiao[1*] (1. School of Mechanical Engineering and Automation, Beihang University, Beijing 100191, China; 2. Department of Electrical Engineering, Beijing Institute of Petro-chemical Technology, Beijing 102617, China). pp 21 – 24

Abstract: The variations of arc pressure and weld characteristics in the welding of 2219, 2A14 and 5A06 aluminum alloys were investigated based on the hybrid ultrahigh frequency pulse current variable polarity gas tungsten arc welding (HPVP-GTAW) process. The experimental results show that compared with the conventional VP-GTAW (variable polarity gas tungsten arc welding) process, arc pressure and weld penetration expressed by the ratio of weld depth to width are enhanced predominantly with the effect of high frequency pulse current. Mechanical properties of welded joints are improved obviously. At the given pulse current amplitude and pulse duty cycle, the welding process is influenced significantly by the pulse current frequency in the range of 10 kHz to 80 kHz. At the given pulse frequency of 40 kHz, arc pressure and weld penetration of welded joints increased by about 90% and 70%, respectively, compared with that of welded joints with no effect of pulse current.

Key words: ultrahigh frequency pulse current; variable polarity gas tungsten arc welding; arc pressure; weld quality

Nanoindentation properties of intermetallic compounds in lead-free solder joints QIN Fei, AN Tong, ZHONG Weixu, LIU Chengyan (College of Mechanical Engineering and Applied Electronics Technology, Beijing University of Technology, Beijing 100124, China). pp 25 – 28, 32

Abstract: The growth of intermetallic compounds (IMC) at the Sn3.0Ag0.5Cu/Cu interface was investigated under isothermal aging temperature of 150 ℃ and aging time of 100, 300, 500 and 1 000 h, respectively. The relationship between the thickness of the IMCs layer and aging time was fitted out, and the growth law of the IMCs layer at Sn3.0Ag0.5Cu/Cu interface under isothermal aging condition was obtained. Mechanical properties of the Cu_6Sn_5 and Cu_3Sn were obtained by a nanoindentation tester. It indicates that with the Cu_6Sn_5 thickness increasing, its Young´s modulus and hardness have no significant change. The Young´s modulus of Cu_3Sn is greater than that of Cu_6Sn_5, but the hardness of Cu_3Sn is lower than that of Cu_6Sn_5. The nanoindentation experiments of the Sn3.0Ag0.5Cu/Cu interfacial zone show that the hardness of Cu, Cu_3Sn, Cu_6Sn_5 and Sn3.0Ag0.5Cu has an order of magnitude that is in sequence $Cu_6Sn_5 > Cu_3Sn > Cu > Sn3.0Ag0.5Cu$.

Key words: electronic packaging; intermetallic compound; nanoindentation; mechanical property

Improvement of corrosion resistance of friction stir welded joint of 7N01-T5 aluminum alloy by micro-arc oxidation LIU Wanhui[1,2], LIU Wenbin[1], BAO Ailian[2] (1. College of Materials Science and Chemical Engineering, Harbin Engineering University, Harbin 150001, China; 2. College of Materials Science and Technology, Heilongjiang Institute of Science and Technology, Harbin 150027, China). pp 29 – 32

Abstract: The ceramic coatings were prepared on surface of friction stir welded joint of 7N01-T5 aluminum alloy by micro arc oxidation technology. The morphology and phase constituent of the micro arc oxidation coatings were studied by SEM, XRD. The corrosion resistance of the friction stir welded joint oxidized and sealed was tested through the neutral salt spray (NSS) test. The results show that micro arc oxidation coating formed on the FSW joint is uniform, and there are many discharge micro-porous like crater and melting, sintering traces on the surface, and which are mainly composed of α-Al_2O_3 and γ-Al_2O_3 phase. Micro arc oxidation ceramic coating has excellent corrosion resistance. Boiling water seal treatment can generate a hydrated alumina, which makes the hole wall inflated and the pore size decreaed, the corrosion resistance of the coatings can be greatly enhanced, and the weight loss is only 2.6 mg after enduring 96 h in NSS test.

Key words: micro arc oxidation; aluminum alloys; friction stir welding; corrosion resistance

Influence of ultrasonic time and pre-clearance on gap-filling behavior of filler metal during ultrasonic-assisted brazing of magnesium alloy LI Hong[1], GENG Yuanyue[1], YAN Jiuchun[2], LI Zhuoxin[1] (1. College of Materials Science and Engineering, Beijing University of Technology, Beijing 100124, China; 2. State Key Laboratory of Advanced Welding and Joining, Harbin Institute of Technology, Harbin 150001, China). pp 33 – 36

Abstract: In order to investigate the influence of ultrasonic on flow behavior of filler metal when the filler metal propagates on the solid/liquid surface in brazing process, the gap-filling behavior of the molten filler metal during ultrasonic-assisted brazing of magnesium alloy was in-situ observed by high-speed video camera. Besides, the gap-filling behavior in unparalleled gaps and brazed joint properties were investigated. When the filler metal fills the gap in the direction parallel to the ultrasonic energy propagation, the dynamic curve of filling-gap distance appears linear relation with the ultrasonic time. And it shows that at the same ultrasonic time, good pre-clearance results in low filling velocity. Along the filler flow direction, the thickness of brazed joint decreases gradually. The filling-gap distance decreases as ultrasonic time increases when filler metal is placed at large gap side. The compactness of the joint is general. The filling-gap distance increases firstly and then decreases with the ultrasonic time increasing when the filler metal is placed at small gap side. In this case, the defects appear in the whole joint. The analysis